

Supplementary Information for: Chemical and isotopic composition of secondary organic aerosol generated by α -pinene ozonolysis

Carl Meusinger¹, Ulrike Dusek^{2,3}, Stephanie M. King^{1,4}, Rupert Holzinger², Thomas Rosenørn^{1,5}, Peter Sperlich^{6,7}, Maxime Julien⁸, Gerald S. Remaud⁸, Merete Bilde^{1,9}, Thomas Röckmann², and Matthew S. Johnson¹

¹Department of Chemistry, University of Copenhagen, DK 2100, Copenhagen Ø, Denmark

²Institute for Marine and Atmospheric research Utrecht (IMAU), Utrecht University, 3584 CC, Utrecht, The Netherlands

³Centre for Isotope Research, Energy and Sustainability Research Institute Groningen, 9747 AG Groningen, The Netherlands

⁴now at: Haldor Topsøe A/S, DK 2800, Kgs. Lyngby, Denmark

⁵Infuser ApS, DK 2200, Copenhagen N, Denmark

⁶Max-Planck Institute for Biogeochemistry, 07745 Jena, Germany

⁷now at: National Institute of Water and Atmospheric Research (NIWA), Wellington 6021, New Zealand

⁸CEISAM, UMR CNRS6230, BP 92208, Nantes 44322 cedex 3, France

⁹now at: Aarhus University, Department of Chemistry, 8000 Aarhus C, Denmark

Correspondence to: C.M. (c.meusinger@gmail.com)

S1 Chamber aerosol characterisation

Figure S1 shows the temporal evolution of SMPS-derived size-distributions and an estimate for total mass concentration, $M_{\text{total}}^{\text{SMPS}}$, derived by assuming spherical particles with a density of 1.2 g/cm³ (Zelenyuk et al., 2008). The charge-correction was not applied to these number-size distributions because the distribution tail at large diameters was beyond the SMPS cut-off diameter. This caused artefacts when applying the charge correction. After the start of VOC-injection, an initial population of particles is formed that grows continuously to sizes of several hundred nanometers within the first hours of the experiment. Multiple populations become visible in Fig. S1 after ca. 5 h that are likely artefacts of multiply-charged particles. As the initial population is growing, it leaves the 'field of view' of the SMPS. As the large particles of the first generation are flushed out of the chamber, less surface area is available for condensation of oxidised vapours and new particle formation is again favoured (at ca. 7 h after start of VOC injection). Roughly one day after injection, new particle formation, condensation upon existing particles, wall losses and the flux of species in and out of the bag are in equilibrium and the measured size distributions stay nearly constant for several days.

Fluctuations in the total mass of the aerosol population (e.g. around 50 h after injection) are most likely due to variations in the VOC injection system. Temporal variability in the size-distribution data originates partly from the fact that no seed particles were present, but such temporal changes in the size-distribution average out over long sampling periods. Panel a in Fig. S2 shows that the SMPS-derived aerosol size distributions is relatively constant over the full sampling time of filters 5 and 6. The two different OH scavengers (experiments A and B) show very similar mass concentrations and the size distributions share the same shape (not shown).

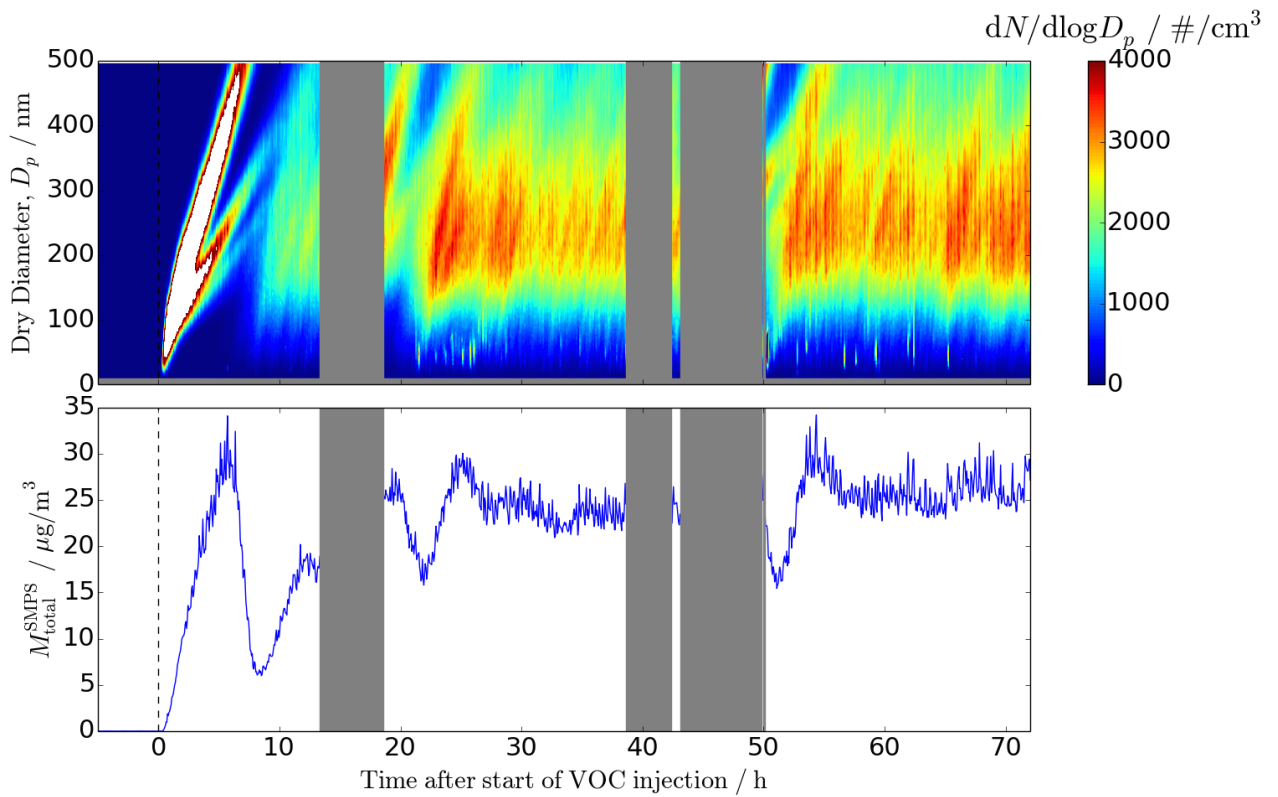


Figure S1. SMPS number size-distribution (10–500 nm range) in $\#/cm^3$ and total mass concentration, $M_{\text{total}}^{\text{SMPS}}$, plotted versus time (for experiment B). Time zero corresponds to the start of VOC injection into the chamber. Filters 5 and 6 sampled between ca. 18 and 42 h and filters 7 and 8 between ca. 48 and 72 h. The SMPS cut-off diameter of 500 nm excludes larger particles, making $M_{\text{total}}^{\text{SMPS}}$ a lower limit. The grey areas denote times when the instrument was offline. The white patch in the initial particle bloom is off the colour scale with values up to $4950/cm^3$.

Panel b in Fig. S2 shows how the generated aerosol particles perform as cloud condensation nuclei. CCN measurements were performed as described previously (King et al., 2012). In short, the aerosol is simultaneously characterized by an SMPS and a CCNC system. The CCNC system itself consists of a DMA, that provides a mono disperse aerosol population for the CCNC and a CPC. The CCNC counts the activated number of particles while the CPC counts the total particle concentration. An automated program allows scanning over the DMA dry diameter and the supersaturation in the CCNC. At each supersaturation, a CCN activity curve is obtained that plots the activated fraction of the aerosol (the ratio of activated aerosol over total concentration) versus the dry diameter of the DMA. Using the size-distribution measured by the SMPS, an inversion is run in order to fit the activity curve (considering multiple charges) and to determine the critical dry diameter, i.e. the size at which particles will activate to be CCN at the given supersaturation. Finally, the program steps through a number of supersaturations in the CCNC

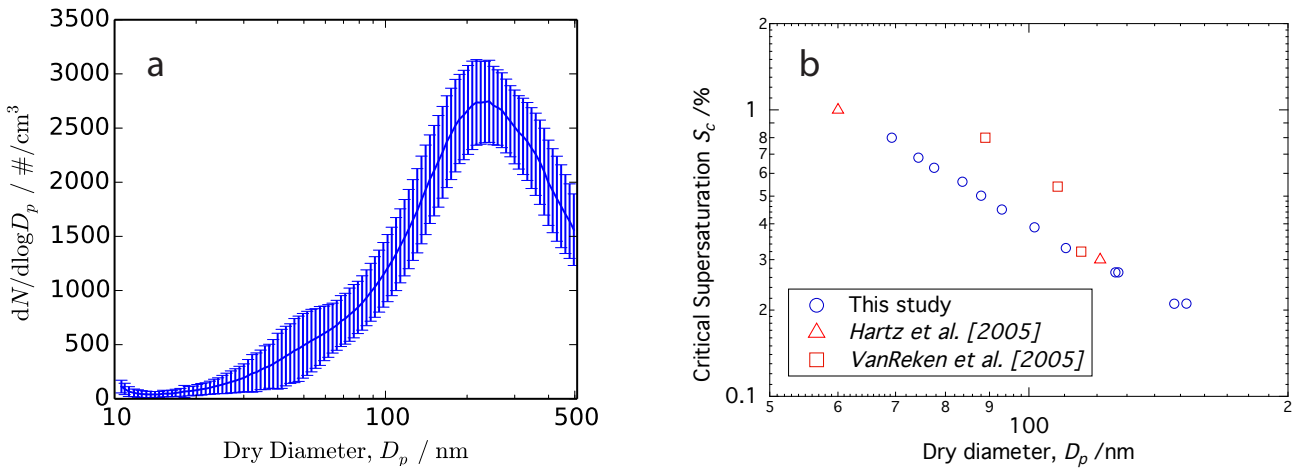


Figure S2. Characterisation of generated aerosol. Panel a shows the average size-distribution and 1- σ standard deviation of the aerosol inside the chamber detected by SMPS during sampling of filters 5 and 6. Panel b shows the CCN activity measured for experiment A. The CCN activity of the generated SOA in the chamber is in agreement with literature data (Hartz et al., 2005; VanReken et al., 2005).

in order to derive a curve like the one presented in Panel b in Fig. S2, where for each supersaturation, the critical dry diameter is given.

S2 Notes on PTR-MS data

S2.1 Fragmentation in the PTR-MS

- 5 Fragmentation of compounds in the PTR-MS is a common artefact (e.g., Holzinger et al., 2010). When such fragmentation occurs, only charged fragments are detected. Protonated water is a common fragment but cannot be observed due to the large background of the primary H_3O^+ ions (19.013 Da). The formation of undetected water means that some oxygen escapes detection, which lowers the reported O:C ratio. If the charged fragments do not coincide in mass with a primary ion at least one of the fragments will be detected by the PTR-MS.
- 10 The arrows in the mass spectrum in Fig. 3 indicate pairs of peaks with a mass difference of 14.016 Da (light arrow) and 18.011 Da (dark arrow). The former can be associated with a CH_2 group while the latter corresponds to the mass of a water molecule. When multiple water molecules are lost this produces series of molecules that are connected this way. In one series ions can originate from the same parent compound entering the PTR-MS. In that case these ions show similar thermograms (similar relative concentrations at different temperature steps). This is the case for the ions the dark arrow connects - the large peak at 169.085 Da and the smaller one at 187.097 Da. The ion concentrations differ by a factor of ca. 10, but their thermograms are similar, which indicates that the actual compound desorbing from the filter has a mass of 187.097 Da. The
- 15

peak at 169.085 Da becomes amplified because of the favoured loss of a water molecule. Ions that are part of a series of the H₂O-loss fragmentation pattern can be numbered relative to each other as $\pm n \times 18.011$ Da. Table 4 and Sect. S4 lists the number n for members of the same series.

Besides the fragmentation that forms water, other fragmentation patterns can occur as well in the PTR-MS. Fragmentation 5 depends on the applied E/N value (Tani et al., 2003; Cappellin et al., 2012), where E is the electric field strength and N the buffer gas number density. E/N describes the drift tube conditions in the PTR-MS and is given in units of Td (1 Td = 1 Townsend = 10^{-17} Vcm²mol⁻¹). Under the employed conditions ($E/N = 124.4$ Td) significant fragmentation is expected for instance for pure gaseous compounds (Tani et al., 2003).

S2.2 Resolution and discrimination of peaks reported in the literature

10 The high mass resolution of the PRT-ToF-MS used in the present study allows more detailed interpretation of the results compared to previous low resolution data obtained with a quadrupole MS. In particular, the PTR-ToF-MS has not been used for measuring the particulate constituents of α -pinene ozonolysis before whereas quadrupole PTR-MS instruments have been used for monitoring the gas-phase (Shilling et al., 2008; Lee et al., 2006) of SOA chamber experiments. These results are difficult to compare, since partitioning coefficients are not known for many organic compounds. The ion with the highest 15 concentration in this study at 169.085 Da will serve as an example: A low resolution peak at 169 Da might be associated with pinonaldehyde (C₁₀H₁₆O₂H⁺), one of the main gas-phase oxidation products of the first reaction step in α -pinene ozonolysis (Camredon et al., 2010). However, the precise molecular weight of pinonaldehyde counting all atoms as primary isotopes, ¹²C, ¹H and ¹⁶O, is 169.123 Da, which differs significantly from the detected peak at 169.085 Da, and thus the compound is not pinonaldehyde. This finding is in line with the low partitioning coefficient reported for pinonaldehyde (Jenkin, 2004) that 20 prevents it from condensing at room temperature. Literature references that reported compounds other than what was identified in this study at the same masses are therefore given in brackets in Table 4 and Sect. S4.

S2.3 Mass scale

As noted earlier the ion at 169.085 Da appears to be in the same water series as the ion with mass 187.097 Da. Besides mechanistic implications, these water series prove useful in checking the performance of the PTR-MS: The presence of water 25 series at high and low masses (e.g. the primary ion and its water clusters and the pair at 169.085 Da and 187.097 Da) ensures that drift in the autoscaling of the PTR-MS mass scale does not cause any ions to be associated with the wrong mass. If the instrument had shown a drift in the mass scale, the drift would scale with the detected mass: a larger deviation would result for heavier ions. However, since the exact difference of the mass of water (18.011 Da) is found on both ends of the mass spectrum, this systematic error can be excluded. Therefore, the given peak assignment is believed to be accurate.

S2.4 Charring

When organic material is heated it pyrolyzes, producing char and gas phase fragments including CO and CO₂, a process commonly referred to as charring. Charring is a known interference with filter-based thermogram methods (Holzinger et al., 2010). The electron affinities of CO and CO₂ are lower than that of water and hence no peaks are detected at the corresponding masses in the PTR-MS. Charring may therefore bias the measurements with implications that include lowered O:C ratios.

S3 Position-specific isotope measurements

Quantitative nuclear magnetic resonance spectrometry (NMR) tuned for isotopic measurement is a tool for quantifying each isotopic isomer of a given molecule (isotopomers): ²H (Martin et al., 2006a, b) or ¹³C (Caytan et al., 2007b). The latest technique, irm-¹³C NMR, is a recent advancement on the more well established irm-²H NMR. It is more of a challenge to quantify the range of variation of ¹³C in natural compounds, which is about ten times less for ¹³C than ²H (about 50‰ and 500‰, respectively, on the δ -scale). The realization of the method required establishing ¹³C NMR conditions to attain a precision of 1‰.

S3.1 NMR acquisition conditions

Table S1 summarises the NMR acquisition parameters used for isotopic ¹³C-NMR. The offset for both ¹³C and ¹H was set at the middle of the frequency range observed. An inverse-gated decoupling technique was used to avoid any Nuclear Overhauser Effect and a cosine adiabatic pulse with appropriate phase cycles was employed as proton decoupling sequence (Tenailleau and Akoka, 2007). A repetition time/inter-pulse delay, greater than ten times the longest longitudinal relaxation delay, T_1 , of the compound was used and the acquisition parameters were adjusted to obtain a signal-to-noise ratio (SNR) > 1500. Free induction decay was submitted to an exponential multiplication inducing a line broadening of 2 Hz. The curve fitting was based on a total-line-shape analyses (deconvolution) carried out with a Lorentzian mathematical model using Perch Software (Perch™ NMR Software, <http://www.perchsolutions.com>). From previous experiments (Bayle et al., 2014; Caytan et al., 2007), SNR > 1500 usually leads to a standard deviation for precision of around 0.2‰. Five spectra were recorded for each measurement: the values reported for each carbon are the mean of the five spectra.

S3.2 Intramolecular ¹³C composition calculations

Briefly, the positional isotopic distribution in a molecule was obtained from the ¹³C mole fractions f_i (where i stands for the C-atom position considered) as follows: $f_i = S_i / S_{\text{tot}}$, where S_i is the ¹³C-signal (i.e. the area under the peak associated with the C-atom at position i , Fig. S3) and S_{tot} is the sum of all ¹³C-signal areas of the molecule. Each S_i was corrected to compensate for the slight loss of intensity caused by satellites (¹³C-¹³C interactions) by multiplying by $(1 + n \times 0.011)$, where n is the number of carbon atoms directly attached to the C-atom position i and 1.1% (= 0.011) is the average natural ¹³C-abundance (see (Silvestre et al., 2009) for a detailed explanation). If F_i denotes the statistical mole fraction (homogeneous ¹³C-

Table S1. NMR acquisition parameters used for isotopic ^{13}C -NMR. T_1 is the longitudinal relaxation delay after addition of the relaxing agent.

Acquisition	Spectral width /ppm	238
	^{13}C offset frequency /ppm	110
	^1H decoupling offset /ppm	4
	Inter-pulse delay /s	32
FID treatment	Line-broadening /Hz	2
	C_1	3.0
	C_2	2.4
	C_3	2.8
	C_4	2.5
	C_5	3.2
	C_6	2.2
	C_7	2.2
	C_8	2.3
	C_9	2.2
	C_{10}	2.3
T_1 /s		

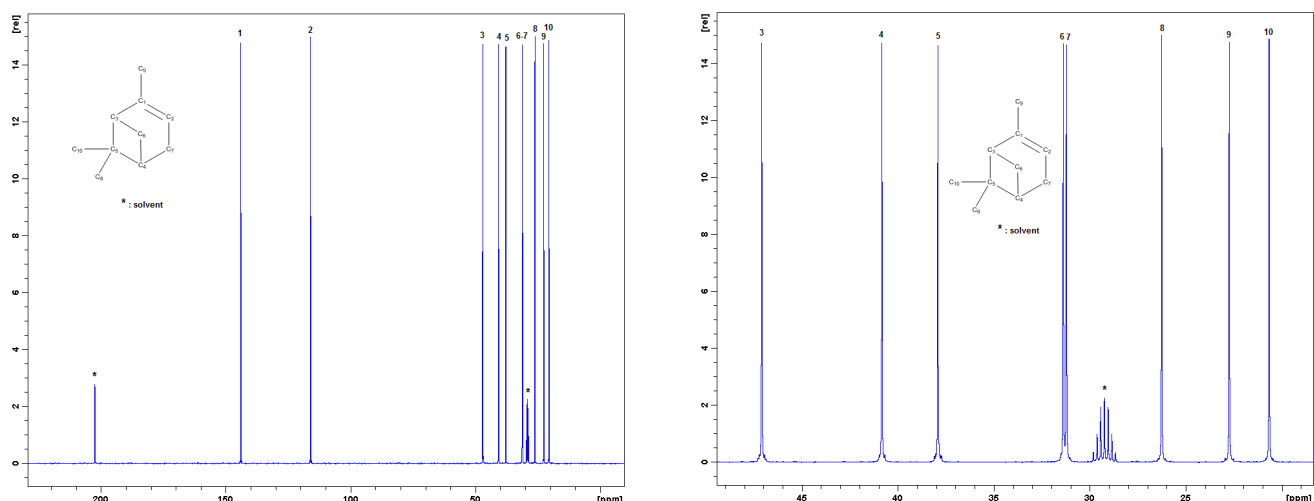


Figure S3. ^{13}C NMR spectrum of α -pinene in acetone-d₆. Left pane: full spectrum, right pane: zoom. The carbon atoms are numbered in relation to decreasing ^{13}C chemical shift in the ^{13}C NMR spectrum.

distribution) at any C-atom position i , then the position-specific relative deviation in the ^{13}C -abundance is $d_i = f_i/F_i - 1$. The values of d_i were converted to delta-values (in ‰) using the isotope composition of the whole molecule, $\delta_{\text{TC}}^{\circ}(^{13}\text{C})$, obtained by IR-MS. Thus, the position-specific compositions are expressed as $\delta_i(^{13}\text{C})$ for each C-atom position of the molecule. Since the peaks of C-6 and C-7 are very close in the ^{13}C NMR spectrum (right panel in Fig. S3), the average of the two corresponding $\delta_i(^{13}\text{C})$ values is given for both. Table S2 shows the discussed quantities for one NMR spectrum of the present data set.

Table S2. Example calculation of $\delta_i(^{13}\text{C})$ of α -pinene from the peak areas in one ^{13}C NMR spectrum. Corrected areas take the interference from satellites into account. See text for more details. Calculations are based on a global $^{13}\text{C}/^{12}\text{C}$ ratio of 0.010808 corresponding to $\delta_{\text{TC}}^{\circ2}(^{13}\text{C}) = -27.7\text{‰}$ with respect to the VPDB scale as measured by IR-MS.

	C ₁	C ₂	C ₃	C ₄	C ₅	C ₆	C ₇	C ₈	C ₉	C ₁₀
Area /a.u.	355.40	360.80	353.30	354.60	347.50	362.50	360.50	361.20	358.60	359.60
Corrected area	367.13	368.74	364.96	366.30	362.79	366.49	364.47	365.17	362.54	363.56
f_i	0.1005	0.1010	0.0999	0.1003	0.0993	0.1003	0.0998	0.1000	0.0993	0.0995
F_i	1/10	1/10	1/10	1/10	1/10	1/10	1/10	1/10	1/10	1/10
f_i/F_i	1.0052	1.0097	0.9993	1.0030	0.9934	1.0035	0.9980	0.9999	0.9927	0.9955
$\delta_i(^{13}\text{C}) / \text{‰}$	-22.5	-18.2	-28.3	-24.7	-34.2	-24.2	-29.7	-27.8	-34.8	-32.1

S4 Full list of ions (filter 6)

The full list of ions detected by PTR-MS from compounds desorbing from filter 6 is printed here and can also be found in the complimentary .csv file 'SI_filter6.csv'.

SI to C. Meusinger et al. Chemical and isotopic composition of secondary organic aerosol generated by alpha-pinene ozonolysis

Full list of ions detected by PTR-MS from compounds desorbing from filter 6 ranked by their concentration

Rank	m/z	Formula	Maximum concentration /ng/m ³	Description Temp. of max. conc. /°C	Description	Literature	H ₂ O relatives
1	169.085	C ₉ H ₁₂ O ₃ H ⁺	267.79	150		a, (c, d)	+1 (187.093 Da, #72), -1 (151.076 Da, #22), -2 (133.065 Da, #202) +1 (99.08 Da, #32)
2	81.07	C ₆ H ₈ OH ⁺	257.57	150	similar to 95.086 Da (#8)		
3	125.096	C ₈ H ₁₂ O ₂ H ⁺	221.48	150		a	
4	43.0172	C ₂ H ₂ O ₂ H ⁺	149.37	150			
5	39.026	C ₃ H ₂ O ₂ H ⁺	132.93	150			
6	155.07	C ₈ H ₁₀ O ₃ H ⁺	127.41	150		a, (b, d)	+1 (173.081 Da, #13)
7	41.038	C ₃ H ₄ OH ⁺	111.32	150		(a)	
8	59.0491	C ₃ H ₆ OH ⁺	110.01	150	Acetone	a, b, c	
9	95.0861	C ₇ H ₁₀ OH ⁺	107.5	150	similar to 81.07 Da (#1)	(d)	
10	127.075	C ₇ H ₁₂ O ₂ H ⁺	69.69	150		a, c	
11	83.0496	C ₅ H ₆ OH ⁺	66.57	150		(a), c	+1 (101.06 Da, #62), -1 (65.04 Da, #96)
12	107.086	C ₈ H ₁₀ OH ⁺	64.79	150		(a)	
13	173.07	C ₈ H ₁₂ O ₂ H ⁺	58.75	150	norpinic acid	b, e, g, (b, e)	-1 (155.07 Da, #6)
14	45.033	C ₂ H ₄ OH ⁺	58.56	100	Acetaldehyde	a, b, c	+1 (63.043 Da, #336)
15	85.065	C ₅ H ₈ OH ⁺	56.71	150		(a)	
16	141.054	C ₇ H ₈ O ₃ H ⁺	56.22	150		a, b, c	+1 (159.065 Da, #63)
17	123.081	C ₈ H ₁₀ O ₂ H ⁺	53.69	150		(a), b, c	-1 (105.072 Da, #58)
18	67.0546	C ₅ H ₆ NH ⁺	50.57	150		(d)	
19	69.0337	C ₄ H ₄ OH ⁺	49.81	150		(a)	
20	69.0699	C ₅ H ₈ B ⁺	43.6	150		(a)	
21	171.065	C ₈ H ₁₀ O ₄ H ⁺	42.34	150	small peak nearby unresolved (norpinic acid?)	a, c, (e, f, g)	-1 (153.055 Da, not listed)
22	151.076	C ₉ H ₁₂ O ₂ H ⁺	42.12	150		(a)	+1 (169.085 Da, #1), +2 (187.093 Da, #72), -1 (133.065 Da, #202)
23	85.029	C ₄ H ₆ O ₂ H ⁺	40.88	200		c	
24	153.091	C ₉ H ₁₂ O ₂ H ⁺	39.97	150		c, (g)	-1 (135.081 Da, #59), -2 (117.070 Da, #152)
25	141.089	C ₉ H ₁₂ O ₂ H ⁺	39.91	150	2,2-Dimethyl-cyclobutyl-1,3-diethanal	a, b, c, g, (g)	
26	71.049	C ₄ H ₆ OH ⁺	39.63	150	MUK & MACR	(a), b	
27	115.076	C ₅ H ₁₀ O ₂ H ⁺	37.17	150		a	-1 (97.0655 Da, #30)
28	181.084	C ₁₀ H ₁₂ O ₃ H ⁺	36.81	150			+1 (199.095, #67), +2 (217.107 Da, #310), -1 (163.076 Da, #107)
29	55.0534	C ₄ H ₆ H ⁺	35.56	150			+1 (73.065 Da, #88)
30	97.0655	C ₆ H ₈ OH ⁺	29.16	150		a	+1 (115.076 Da, #27)
31	170.089	13C ₈ H ₁₂ O ₂ H ⁺	27.96	150	13C of #2	(a)	+1 (188.096, #219), -1 (152.080, #120), -2 (unresolved)
32	99.0807	C ₆ H ₁₀ OH ⁺	27.48	150		(a)	-1 (81.07 Da, #2)
33	165.09	C ₁₀ H ₁₂ O ₂ H ⁺	26.62	350		a	
34	79.0547	C ₅ H ₆ H ⁺	26.36	150		a	
35	57.0698	C ₄ H ₈ H ⁺	26.3	150			
36	183.094	C ₁₀ H ₁₄ O ₃ H ⁺	26	150	C ₁₀ HCO, 4-Oxopinaldehyde	a, e, f, g, h	+1 (201.117 Da, #239), +2 (not resolved)
37	83.085	C ₆ H ₁₀ OH ⁺	25.48	150		(a)	
38	109.101	C ₈ H ₁₂ H ⁺	25.45	150			
39	125.06	C ₇ H ₈ O ₂ H ⁺	25.36	150		a, c	not well resolved
40	151.111	C ₁₀ H ₁₄ O ₄ H ⁺	24.1	150			
41	138.04	C ₇ H ₆ O ₃ H ⁺	22.68	150		a, c	+1 (157.05 Da, #50)
42	93.0697	C ₇ H ₈ H ⁺	21.98	150			
43	109.066	C ₇ H ₈ OH ⁺	21.75	150			
44	126.094	13C ₇ H ₈ OH ⁺	20.59	150		c	+1 (75.044 Da, #48)
45	57.0337	C ₃ H ₄ OH ⁺	20.41	100		a, c	
46	47.0126	C ₂ H ₂ O ₂ H ⁺	19.99	150			
47	95.0576	C ₅ H ₆ N ₂ H ⁺	19.81	150		a	-1 (57.033 Da, #45)
48	75.044	C ₃ H ₆ O ₂ H ⁺	19.79	100		a, c	
49	129.055	C ₅ H ₈ O ₃ H ⁺	19.64	150		c, h	-1 (139.04 Da, #41)
50	157.05	C ₇ H ₈ O ₄ H ⁺	18.8	150	CO ₂ SC ₆ CHO	f, g	
51	171.098	13C ₁₁ H ₁₁ N ₁ H ⁺	18.75	150	norpinic acid (?) , C ₉ H ₁₄ O ₃ H ⁺	a, c	+1 (185.118 Da, #116), -1 (149.098 Da, #134)
52	119.085	C ₆ H ₁₀ OH ⁺	17.71	150			
53	143.07	C ₇ H ₁₀ O ₃ H ⁺	17.46	200		a, c	
54	167.104	C ₉ H ₁₄ O ₂ N ₂ H ⁺	17.17	150			+1 (185.118 Da, #116), -1 (149.098 Da, #134)
55	123.114	C ₉ H ₁₄ OH ⁺	15.99	150		a, c	-1 (121.068, #101), +1 (157.087, #64)
56	138.075	C ₈ H ₁₂ O ₂ H ⁺	15.98	150		a, b, c	
57	113.06	C ₅ H ₈ O ₂ H ⁺	15.96	150		b	+1 (123.081 Da, #17)
58	105.071	C ₈ H ₈ H ⁺	15.86	150			+1 (153.091 Da, #24), -1 (117.070 Da, #152)
59	135.081	C ₉ H ₁₀ O ₄ H ⁺	15.02	150		c	
60	61.0286	C ₂ H ₄ O ₂ H ⁺	14.8	150	Acetic acid	a, c	
61	87.0445	C ₄ H ₆ O ₂ H ⁺	14.59	150		c	
62	101.06	C ₅ H ₈ O ₂ H ⁺	14.4	150		a, c	-1 (83.0496 Da, #11), -2 (65.04 Da, #96)
63	159.063	C ₇ H ₁₀ O ₄ H ⁺	14.27	150	C ₈ H ₁₀	b, h	-1 (141.054 Da, #16)
64	157.083	C ₈ H ₁₂ O ₃ H ⁺	13.94	150	C ₇ H ₁₀	h	-1 (139.075 Da, #56), -2 (121.068 Da, #101)
65	111.08	C ₇ H ₁₀ OH ⁺	13.8	150		a, b	
66	55.0182	C ₂ H ₂ O ₂ H ⁺	13.36	150			
67	199.095	C ₅ H ₁₄ O ₂ N ₂ H ⁺	12.87	150	oxopinaldehyde, keto-pinonic acid	e, g	-1 (181.084 Da, #28), -2 (163.076 Da, #107), +1 (217.107 Da, #310)
68	82.0738	13C ₅ H ₈ OH ⁺	12.15	150		b	
69	156.074	13C ₇ H ₈ OH ⁺	11.91	150		a, b, c	
70	145.05	C ₆ H ₈ O ₄ H ⁺	11.9	150		e, f, g, h	-1 (169.085 Da, #1), -2 (151.076 Da, #22), -3 (133.065 Da, #202)
71	111.045	C ₆ H ₈ O ₂ H ⁺	11.87	150			-1 (77.040, #213)
72	187.093	C ₉ H ₁₄ O ₄ H ⁺	11.37	150	pinic acid, 10-OH norpinic acid, PINIC	a	
73	95.0497	C ₆ H ₁₀ OH ⁺	11.09	150		a, b, c	-1 (95.020 Da, #144)
74	139.109	C ₉ H ₁₄ O ₄ H ⁺	10.82	150	nopinone (?)	a, f	-1 (121.103 Da, #100)
75	81.0356	C ₅ H ₈ OH ⁺	10.49	150		c	
76	97.058	no match	10.35	150			
77	137.095	C ₉ H ₁₂ O ₂ H ⁺	9.87	150			
78	111.053	C ₅ H ₆ O ₂ N ₂ H ⁺	9.67	150		a	
79	73.0283	C ₃ H ₆ O ₂ H ⁺	9.43	150		a, c	
80	113.024	C ₅ H ₄ O ₃ H ⁺	9.18	200		a, b, c	
81	53.0385	C ₄ H ₄ HH ⁺	8.95	150			
82	99.0444	C ₅ H ₆ O ₂ H ⁺	8.83	150		c	
83	96.09	13C ₆ H ₁₀ H ⁺	8.82	150			

Rank	m/z	Formula	Maximum concentration /ng/m3	Description Temp. of max. conc. /°C	Description	Literature	H2O relatives
84	137.06	C8H8O2H+	8.23	150			
85	109.058	C2H8O3N2H+	8.16	150			
86	93.062	no match	8.11	150			
87	129.087	no match	8.06	150	a		
88	73.0648	C4H8OH+	8.05	150	a	-1 (55.0534 Da, #29)	
89	99.0085	C4H10O3H+	8.01	200			
90	128.078	13CC6H10O2H+	7.65	150			
91	68.9974	no match	7.56	150			
92	95.042	no match	7.51	150			
93	214.087	C13H11O2N2H+	7.45	150			
94	167.074	C9H10O3H+	7.33	150			
95	97.029	C5H4O2H+	7.33	150	a, c		
96	65.039	C5H4H+	7.32	150		+1 (83.0496 Da, #11), +2 (101.06 Da, #62)	
97	123.052	no match	7.27	150			
98	197.079	C10H12O4H+	7.23	150			
99	173.147	no match	6.88	150			
100	121.101	C9H12H+	6.86	150		+1 (139.109 Da, #74)	
101	121.065	C8H8OH+	6.86	150		+1 (139.075 Da, #56), +2 (157.080, #64)	
102	127.037	C6H6O3H+	6.62	150	c		
103	85.0993	C6H12H+	6.44	150			
104	651.119	no match	6.37	150			
105	185.079	C9H12O4H+	6.35	150	c		
106	725.102	no match	6.26	150			
107	163.075	C10H10O2H+	5.95	150	b	+1 (181.084 Da, #28), +2 (199.095, #67), +3 (217.107 Da, #310)	
108	82.0718	13CC5H8H+	5.95	150			
109	124.084	13CC7H10OH+	5.84	150			
110	108.089	13CC7H10H+	5.8	150			
111	91.0549	C7H6H+	5.76	150			
112	125.023	C6H6O3H+	5.67	150			
113	174.083	13CC7H12O4H+	5.67	150	C8902		h
114	107.049	C7H6OH+	5.42	150			
115	33.0327	C4H4OH+	5.32	150			
116	185.117	C10H16O3H+	5.31	150	Methanol		
117	172.068	13CC7H10O4H+	5.1	150	pinonic acid, OH-pinonaldehyde, PINONIC, C107OH, C109OH	a, e, f, g, h	-1 (167.105 Da, #54), -2 (149.098 Da, #134)
118	101.052	no match	4.77	150			
119	142.058	13CC6H8O3H+	4.69	150			
120	152.079	13CC8H10O2H+	4.54	150		+1 (170.089, #31), +2 (188.096, #219), -1 (unresolved)	
121	171.148	C9H18O2N2H+	4.49	150			
122	43.0584	C3H6H+	4.47	150			
123	115.04	C5H6O3H+	4.4	150	a, c		
124	40.0256	13CC2H2OH+	4.29	150			
125	154.093	13CC8H12O2H+	4.29	150			
126	182.088	13CC9H12O3H+	4.28	150		+1 (200.097 Da, #197), +2 (218.109 Da, not resolved)	
127	70.0734	13CC4H8H+	4.12	150			
128	71.0812	no match	4.06	150			
129	60.0521	13CC2H6OH+	4.02	150			
130	123.043	C7H6O2H+	3.99	150			
131	183.163	no match	3.95	150			
132	141.008	C2H4O7H+	3.94	150			
133	84.0525	13CC4H6OH+	3.88	150			
134	149.095	C10H12O2H+	3.84	150	methylchavicol (Holz 2005)	b	+1 (167.105, #54), +2 (185.118 Da, #116)
135	211.093	C6H14O4DN2H+	3.81	150			
136	42.0414	13CC2H4H+	3.72	150			
137	142.093	13CC7H12O2H+	3.65	150			
138	741.107	no match	3.62	150			
139	121.098	no match	3.54	150			
140	44.0205	13CH2O2H+	3.31	150			
141	653.119	no match	3.28	150			
142	86.068	13CC4H8OH+	3.28	150			
143	184.103	13CC9H14O3H+	3.22	150			
144	95.0141	C5H2O2H+	3.2	200		+1 (113.024 Da, #80)	
145	145.089	no match	3.16	150			
146	166.094	13CC9H12O2H+	3.13	350			
147	87.0798	C5H10OH+	3.02	150	MBO (holz 2005)	a, b	
148	109.031	C6H4O2H+	2.96	150			
149	101.095	C6H12OH+	2.95	150			
150	99.0371	no match	2.95	150			
151	101.024	C4H4O3H+	2.95	150	c		
152	117.069	C3H8H+	2.87	150		+1 (135.081 Da, #59), +2 (153.091 Da, #24)	
153	103.04	C4H6O3H+	2.86	100			
154	152.112	13CC4H14O3N2H+	2.85	150			
155	149.024	C8H4O3H+	2.83	150	c		
156	110.069	13CC6H8OH+	2.6	150			
157	96.0531	13CC5H6OH+	2.57	150			
158	126.063	13CC6H8O2H+	2.54	150			
159	429.077	no match	2.5	150			
160	68.058	13CC4H6OH+	2.48	150			
161	83.0138	C4H2O2H+	2.47	150			
162	42.9985	no match	2.43	150			
163	147.08	C10H10O4H+	2.41	150			
164	110.105	13CC7H12H+	2.35	150			
165	103.048	C3H6O2N2H+	2.34	100			
166	70.038	13CC3H4OH+	2.3	150			
167	116.08	13CC5H10O2H+	2.27	150			
168	71.0136	C3H2O2H+	2.27	200			

Rank	m/z	Formula	Maximum concentration /ng/m3	Description Temp. of max. conc. /°C	Description	Literature	H2O relatives
169	55.0103	no match	2.24	150			
170	652.095	no match	2.24	150			
171	187.068	no match	2.23	150			
172	72.052	13CC3H6OH+	2.23	150			
173	94.0733	13CC5H8OH++	2.23	150			
174	667.131	no match	2.22	150			
175	117.061	no match	2.22	150			
176	133.097	C5H12O2N2H+	2.18	150			
177	215.09	C10H14O5H+	2.15	150			
178	652.128	no match	2.11	150			
179	187.06	C8H10O5H+	2.11	200			
180	98.0687	13CC5H8OH-	2.1	150			
181	93.039	C6H4OH+	2.08	150			
182	168.107	13CC9H14O2H+	2.02	150			
183	31.017	C12O4H+	2.01	150	Formaldehyde		
184	100.084	13CC5H10OH+	1.98	150			
185	119.05	C6H6OH-	1.87	150			
186	86.0328	13CC3H4O2H2+	1.87	200			
187	140.044	13CC5H6O3H++	1.86	150			
188	120.088	13CC8H10H+	1.85	150			
189	168.676	no match	1.83	150			
190	124.819	no match	1.81	150			
191	159.131	no match	1.79	150			
192	239.23	no match	1.77	150			
193	229.102	C6H16O7N2H+	1.76	150			
194	56.0575	13CC3H6H+	1.71	150			
195	84.0884	13CC5H5OH+	1.71	150			
196	277.137	C11H20O6N2H+	1.68	200			
197	200.097	13CC4H4O4O2NH+	1.66	150	C10H15O4H+, C10T02		
198	149.062	13CC4H9O4OH+	1.64	150			
199	136.084	13CC8H10OH+	1.63	150			
200	80.0576	13CC5H6H+	1.62	150			
201	119.036	C4H6O4H+	1.61	150			
202	133.065	C9H8OH-	1.6	150	a	+1 (151.076 Da, #22), +2 (169.085 Da, #1), +3 (187.093 Da, #72)	
203	654.111	no match	1.57	150			
204	199.161	no match	1.56	150			
205	140.078	13CC7H10O2H+	1.56	150			
206	80.9047	no match	1.56	150			
207	154.934	no match	1.55	150			
208	179.07	C10H10O3H+	1.55	350	b	-1 (161.072, #401)	
209	121.028	C7H4O2H-	1.51	150			
210	213.074	C10H12O5H+	1.5	200	b	-1 (195.068 Da, #265)	
211	130.058	13CC5H8O3H++	1.49	150			
212	103.083	no match	1.48	200			
213	77.0394	C5H4H+	1.46	150		+1 (95.0497 Da, #73)	
214	80.938	no match	1.43	150			
215	106.074	13CC7H9H++	1.43	150			
216	144.073	13CC6H10O3H+	1.42	200			
217	371.092	no match	1.41	150			
218	158.086	no match	1.4	150			
219	188.096	no match	1.39	150	C9T02		
220	179.098	no match	1.37	350	b	-1 (170.089, #31), -2 (152.080, #120), -3 (unresolved)	
221	158.053	13CC5H8O4H+	1.36	150			
222	80.9795	no match	1.34	150			
223	46.0305	C9OHNH-	1.33	150			
224	59.0086	no match	1.32	150			
225	669.137	no match	1.27	150			
226	257.246	C16H32O2H+	1.27	150			
227	223.097	C12H14O4H+	1.27	150			
228	355.063	no match	1.26	150			
229	145.104	13CC6H13O2NH+	1.26	150			
230	65.022	13CC3H6H+	1.25	150			
231	209.184	C14H24O4H-	1.23	100			
232	160.069	13CC6H10O4H+	1.22	150			
233	193.117	C7H16O4N2H+	1.22	150			
234	112.083	13CC5H10OH-	1.2	150			
235	140.114	13CC8H14O4H+	1.19	150			
236	285.268	no match	1.17	150			
237	154.926	no match	1.16	150			
238	279.155	C11H22O6N2H+	1.16	200			
239	201.117	no match	1.13	150	C10T00H, C109O0H, HOPINONIC, C108OH, 10-OH pinonic acid, OH-pinaldehyde e, f, g, h	-1 (183.099 Da, #36) +1 (not resolved)	
240	267.256	no match	1.13	150			
241	80.8614	no match	1.12	150			
242	112.048	13CC5H6O2H++	1.11	150			
243	198.084	13CC9H12O4H+	1.09	150			
244	131.07	C5H10O3H-	1.09	150			
245	189.084	C7H12O4N2H+	1.09	150			
246	114.065	13CC5H8O2H++	1.09	150			
247	101.016	no match	1.09	150			
248	122.104	13CC8H12H+	1.08	150			
249	138.098	13CC8H12O4H+	1.06	150			
250	102.062	13CC4H8O2H+	1.05	150			
251	105.036	13CC2H5O3NH+	1.04	150			
252	168.08	C12H9N+-	1.03	150			
253	168.649	no match	0.99	150			

Rank	m/z	Formula	Maximum concentration /ng/m ³	Description Temp. of max. conc. /°C	Description	Literature	H2O relatives
254	195.095	C6H14O5N2H ⁺	0.98	150			
255	257.226	C19H28H ⁺	0.98	150			
256	80.9714	no match	0.97	150			
257	154.711	no match	0.97	150			
258	124.785	no match	0.96	150			
259	138.066	13C3CH7H2O2H ⁺	0.94	150			
260	269.165	C17H20ON2H ⁺	0.92	150			
261	82.0405	no match	0.92	150			
262	122.068	13C3CH7HOH ⁺	0.9	150			
263	74.0636	no match	0.89	150			
264	133.056	no match	0.89	150			
265	195.068	C10H10O4H ⁺	0.89	200			
266	131.088	13C5H11O2NH ⁺	0.89	150			
267	150.726	no match	0.86	150			
268	131.034	C5H6O4H ⁺	0.86	150			
269	201.076	C9H12O5H ⁺	0.84	150			
270	110.993	C12O6H ⁺	0.83	150			
271	431.076	no match	0.81	150			
272	140.928	no match	0.81	150			
273	578.098	no match	0.79	100			
274	164.077	13C3CH9H10O2H ⁺	0.78	150			
275	58.072	13C3CH8H ⁺	0.77	150			
276	186.081	13C3H11O2G6N2H ⁺	0.76	150			
277	124.794	no match	0.76	150			
278	94.8514	no match	0.76	150			
279	68.97	no match	0.76	150			
280	202.076	13C3H3H12O7N2H ⁺	0.75	150			
281	87.01	C3H2O3H ⁺	0.75	150			
282	186.117	no match	0.74	150			
283	241.107	C12H16O5H ⁺	0.74	200			
284	42.9903	no match	0.73	150			
285	94.8927	no match	0.73	150			
286	58.0365	13C3H2H4OH ⁺	0.72	100			
287	94.9561	no match	0.71	150			
288	98.0605	C5H7ONH ⁺	0.71	150			
289	150.098	13C3H9H12O2H ⁺	0.71	150			
290	577.101	no match	0.71	100			
291	146.053	13C5H8H4O4H ⁺	0.71	150			
292	66.0437	13C4H4M ⁺	0.7	150			
293	158.028	13C3H4H4O4N2H ⁺	0.69	150			
294	76.0484	13C3H2H6O2H ⁺	0.69	100			
295	88.0483	13C3H6H6O2H ⁺	0.69	150			
296	204.119	13C3C11H14O2N2H ⁺	0.68	150			
297	89.0233	C3H4O3H ⁺	0.68	150			
298	219.112	C12H14O2N2H ⁺	0.67	350			
299	124.049	13C3H6H6O2H ⁺	0.66	150			
300	116.106	C6H13ONH ⁺	0.66	150			
301	154.685	no match	0.66	150			
302	193.088	13C3GH13O5NH ⁺	0.66	350			
303	108.962	no match	0.66	150			
304	447.088	no match	0.65	150			
305	114.091	C6H11O1NH ⁺	0.65	150			
306	211.196	no match	0.64	150			
307	227.123	C7H18O6N2H ⁺	0.64	200			
308	100.047	13C3H4H6O2H ⁺	0.63	150			
309	231.095	C9H14O5N2H ⁺	0.63	350			
310	217.107	C10H16O5H ⁺	0.63	350			
311	58.0803	no match	0.63	150			
312	225.135	C9H12O6H ⁺	0.62	150			
313	577.071	no match	0.62	100			
314	209.109	C14H12N2H ⁺	0.62	150			
315	205.113	no match	0.61	350			
316	175.108	C7H14O4N2H ⁺	0.61	150			
317	161.098	C11H12O2H ⁺	0.61	350			
318	212.097	13C3C5H14O4N2H ⁺	0.61	150			
319	223.119	C9H18O6H ⁺	0.61	150			
320	175.08	13C3GH11O4NH ⁺	0.61	150			
321	201.092	C13H12O2H ⁺	0.61	150			
322	172.15	13C9H18ON2H ⁺	0.6	150			
323	295.147	C11H22O7N2H ⁺	0.6	200			
324	108.054	13C3H6H6O ⁺	0.6	150			
325	199.17	C12H22O2H ⁺	0.6	150			
326	430.084	no match	0.59	150			
327	140.919	no match	0.59	150			
328	210.117	13C3GH16O5N2H ⁺	0.59	150			
329	94.902	no match	0.59	150			
330	94.9478	no match	0.59	150			
331	130.09	13C3GH11O2H ⁺	0.59	150			
332	45.006	no match	0.59	100			
333	177.115	C8H16O4H ⁺	0.58	350			
334	229.214	C14H28D2H ⁺	0.57	150			
335	56.021	13C2H2OH ⁺	0.57	150			
336	63.0429	C2H6O2H ⁺	0.57	150			
337	239.137	C12H18O3N2H ⁺	0.57	150			
338	168.668	no match	0.57	150			

b, +1 (213.074 Da, #210)

f, h, -1 (199.095, #67), -2 (181.084 Da, #28), -3 (163.076 Da, #107)

-1 (45.033 Da, #14)

Rank	m/z	Formula	Maximum concentration /ng/m ³	Description Temp. of max. conc. /°C	Description	Literature	H ₂ O relatives
339	207.099	C7H14O5N2H ⁺	0.57	350			
340	225.109	C7H16O6N2H ⁺	0.56	150			
341	114.027	13CC4H4O3NH ⁺	0.56	200			
342	190.104	13CC1OH12O2N2H ⁺	0.56	150			
343	68.9359	no match	0.55	150			
344	89.0603	C4H8O2H ⁺	0.55	150			
345	430.062	no match	0.54	150			
346	579.095	no match	0.54	100			
347	205.089	13CC7H13O5NH ⁺	0.53	350			
348	42.933	no match	0.53	150			
349	146.075	no match	0.53	150			
350	299.063	no match	0.53	150			
351	47.046	no match	0.53	150	ethanol		
352	243.129	C12H18O5H ⁺	0.51	150			
353	216.09	13CC4H14O7N2H ⁺	0.51	150	C10802		
354	297.155	C12H24O8H ⁺	0.51	150			
355	117.024	no match	0.5	150			
356	243.231	C15H30O2H ⁺	0.5	150			
357	92.0581	13CC6H6H ⁺	0.5	150			
358	209.165	C12H20O2N2H ⁺	0.49	100			
359	257.128	C15H16O2N2H ⁺	0.49	150			
360	42.9787	no match	0.49	150			
361	593.15	no match	0.48	100			
362	131.08	C5H10O2N2H ⁺	0.48	150			
363	81.2891	no match	0.48	150			
364	102.092	C5H11O1NH ⁺	0.47	150			
365	207.13	no match	0.47	350			
366	98.029	13CC4H4O2H ⁺	0.47	150			
367	267.132	C13H18O4N4H ⁺	0.46	150			
368	41.007	no match	0.46	150			
369	68.0501	C4H5NH ⁺	0.46	150			
370	188.064	13CC7H11O5H ⁺	0.45	150			
371	58.9874	no match	0.45	150			
372	258.25	13CC15H32O2H ⁺	0.44	150			
373	180.64	no match	0.44	150			
374	209.083	13CC6H13O4NH ⁺	0.44	200			
375	215.181	C16H22H ⁺	0.44	150			
376	281.143	C15H20O5H ⁺	0.44	150			
377	225.043	13CC5H9O3NH ⁺	0.43	150			
378	356.066	no match	0.42	150			
379	58.924	no match	0.42	150			
380	45.9922	O2N ⁺	0.42	150			
381	122.804	no match	0.41	150			
382	42.9554	no match	0.41	150			
383	150.028	13CC7H4O3JH ⁺	0.4	150			
384	94.837	no match	0.4	150			
385	241.178	C14H24O3H ⁺	0.4	150			
386	112.041	C5H5O2NH ⁺	0.4	150			
387	74.0313	13CC2H4O2H ⁺	0.4	150			
388	42.9091	no match	0.4	150			
389	261.137	no match	0.4	350			
390	225.216	no match	0.39	150			
391	283.147	C17H18O2N2H ⁺	0.39	150			
392	38.9477	no match	0.39	150			
393	357.062	no match	0.39	150			
394	106.83	no match	0.38	150			
395	44.049	C2H5NH ⁺	0.38	150			
396	201.163	C15H20H ⁺	0.37	150			
397	62.0316	13CC4H4O2H ⁺	0.36	150			
398	42.0333	C2H5NH ⁺	0.36	150			
399	46.991	O215N ⁺	0.36	150			
400	81.287	no match	0.35	150			
401	161.059	C10H18O2H ⁺	0.35	150			
402	58.9788	no match	0.35	150			
403	227.096	C12H18O4H ⁺	0.35	150			
404	255.137	C17H18O2H ⁺	0.34	150			
405	251.147	C11H22O6H ⁺	0.34	150			
406	42.9691	no match	0.34	150			
407	243.119	C7H18O7N2H ⁺	0.34	150			
408	43.1766	no match	0.34	150			
409	201.176	no match	0.34	150			
410	297.077	13CC12H13O7N7H ⁺	0.34	150			
411	283.24	C16H30O2N2H ⁺	0.34	150			
412	124.041	C6H5O2NH ⁺	0.33	150			
413	240.236	no match	0.33	150			
414	271.14	C10H22O8H ⁺	0.33	150			
415	275.246	C18H30N2H ⁺	0.32	150			
416	237.137	C16H16N2H ⁺	0.32	200			
417	44.0124	CHONH ⁺	0.31	150			
418	40.9457	no match	0.31	150			
419	432.075	no match	0.31	150			
420	194.098	C14H11NH ⁺	0.31	150			
421	448.087	no match	0.3	150			
422	192.104	13CC6H14O4N2H ⁺	0.3	150			
423	82.8441	no match	0.29	150			

+1 (179.07 Da, #208)

Rank	m/z	Formula	Maximum concentration /ng/m3	Desorption Temp. of max. conc. /°C	Description	Literature	H2O relatives
424	253.178	$\text{C}1\text{CC}1\text{H}2\text{1NH}^+$	0.29	150			
425	219.168	$\text{C}1\text{OH}2\text{2O3N2H}^+$	0.29	350			
426	287.148	$\text{C}1\text{H}4\text{22O6H}^+$	0.28	200			
427	373.088	no match	0.27	150			
428	235.165	$\text{C}1\text{OH}2\text{2O4N2H}^+$	0.27	150			
429	191.176	$\text{C}9\text{H}2\text{2O2N2H}^+$	0.27	100			
430	237.212	no match	0.27	150			
431	41.0866	no match	0.27	150			
432	594.142	no match	0.26	100			
433	268.259	no match	0.26	150			
434	210.193	$\text{C}3\text{C}1\text{H}3\text{2A4O}^+$	0.25	100			
435	245.157	$\text{C}1\text{S}1\text{H}6\text{O3H}^+$	0.25	350			
436	280.16	$\text{C}3\text{C}1\text{H}4\text{22O6N2H}^+0.25$		150			
437	108.804	no match	0.23	150			
438	179.175	no match	0.23	350			
439	221.076	$\text{C}7\text{H}1\text{2O6N2H}^+$	0.23	250			
440	257.098	$\text{C}7\text{H}1\text{6O6N2H}^+$	0.22	150			
441	259.185	no match	0.22	150			
442	242.12	$\text{C}3\text{C}1\text{H}1\text{6O6N2H}^+0.22$		200			
443	120.047	$\text{C}3\text{C}2\text{H}6\text{O3N2H}^+$	0.2	150			
444	303.273	$\text{C}3\text{C}1\text{H}4\text{3S}1\text{O3N}3\text{H}^+$	0.2	150			
445	221.148	$\text{C}9\text{H}2\text{O4N2H}^+$	0.19	150			
446	286.275	$\text{C}1\text{7H}3\text{S}1\text{O2N}2\text{H}^+$	0.17	150			
447	192.137	$\text{C}1\text{2H}1\text{7O}2\text{NH}^+$	0.15	150			
448	358.06	no match	0.14	150			
449	120.039	$\text{C}3\text{C}3\text{H}6\text{O4H}^+$	0.13	150			
450	260.186	$\text{C}1\text{3H}2\text{5O4N}4\text{H}^+$	0.11	150			
451	581.1	no match	0.1	100			

References

- Bayle, K., Gilbert, A., Julien, M., Yamada, K., Silvestre, V., Robins, R. J., Akoka, S., Yoshida, N., and Reaud, G. S.: Conditions to obtain precise and true measurements of the intramolecular ^{13}C distribution in organic molecules by isotopic ^{13}C nuclear magnetic resonance spectrometry, *Anal. Chim. Acta.*, 846, 1–7, doi:10.1016/j.aca.2014.07.018, <http://www.sciencedirect.com/science/article/pii/S0003267014008630>, 2014.
- Camredon, M., Hamilton, J. F., Alam, M. S., Wyche, K. P., Carr, T., White, I. R., Monks, P. S., Rickard, A. R., and Bloss, W. J.: Distribution of gaseous and particulate organic composition during dark alpha-pinene ozonolysis, *Atmos. Chem. Phys.*, 10, 2893–2917, doi:10.5194/acp-10-2893-2010, <http://www.atmos-chem-phys.net/10/2893/2010/>, 2010.
- Cappellin, L., Karl, T., Probst, M., Ismailova, O., Winkler, P. M., Soukoulis, C., Aprea, E., Märk, T. D., Gasperi, F., and Biasioli, F.: On Quantitative Determination of Volatile Organic Compound Concentrations Using Proton Transfer Reaction Time-of-Flight Mass Spectrometry, *Environ. Sci. Technol.*, 46, 2283–2290, doi:10.1021/es203985t, <http://pubs.acs.org/doi/abs/10.1021/es203985t>, 2012.
- Caytan, E., Reaud, G. S., Tenailleau, E., and Akoka, S.: Precise and accurate quantitative ^{13}C NMR with reduced experimental time, *Talanta*, 71, 1016–1021, doi:10.1016/j.talanta.2006.05.075, 2007b.
- Caytan, E., Botosoa, E. P., Silvestre, V., Robins, R. J., Akoka, S., and Reaud, G. S.: Accurate Quantitative ^{13}C NMR Spectroscopy: Repeatability over Time of Site-Specific ^{13}C Isotope Ratio Determination, *Anal. Chem.*, 79, 8266–8269, doi:10.1021/ac070826k, 2007.
- Hartz, K. E. H., Rosenørn, T., Ferchak, S. R., Raymond, T. M., Bilde, M., Donahue, N. M., and Pandis, S. N.: Cloud condensation nuclei activation of monoterpane and sesquiterpene secondary organic aerosol, *J. Geophys. Res.*, 110, D14 208, doi:10.1029/2004JD005754, <http://www.agu.org/pubs/crossref/2005/2004JD005754.shtml>, 2005.
- Holzinger, R., Kasper-Giebl, A., Staudinger, M., Schauer, G., and Röckmann, T.: Analysis of the chemical composition of organic aerosol at the Mt. Sonnblick observatory using a novel high mass resolution thermal-desorption proton-transfer-reaction mass-spectrometer (hr-TD-PTR-MS), *Atmos. Chem. Phys.*, 10, 10 111–10 128, doi:10.5194/acp-10-10111-2010, <http://www.atmos-chem-phys.net/10/10111/2010/>, 2010a, 2010-1, 2010.
- Jenkin, M. E.: Modelling the formation and composition of secondary organic aerosol from alpha- and beta-pinene ozonolysis using MCM v3, *Atmos. Chem. Phys.*, 4, 1741–1757, doi:10.5194/acp-4-1741-2004, <http://www.atmos-chem-phys.net/4/1741/2004/>, 2004.
- King, S. M., Butcher, A. C., Rosenørn, T., Coz, E., Lieke, K. I., de Leeuw, G., Nilsson, E. D., and Bilde, M.: Investigating Primary Marine Aerosol Properties: CCN Activity of Sea Salt and Mixed Inorganic–Organic Particles, *Environ. Sci. Technol.*, 46, 10 405–10 412, doi:10.1021/es300574u, <http://pubs.acs.org/doi/abs/10.1021/es300574u>, 2012.
- Lee, A., Goldstein, A. H., Keywood, M. D., Gao, S., Varutbangkul, V., Bahreini, R., Ng, N. L., Flagan, R. C., and Seinfeld, J. H.: Gas-phase products and secondary aerosol yields from the ozonolysis of ten different terpenes, *J. Geophys. Res.*, 111, D07 302, doi:10.1029/2005JD006437, <http://www.agu.org/pubs/crossref/2006/2005JD006437.shtml>, 2006.
- Martin, G. J., Martin, M. L., and Reaud, G.: SNIF-NMR—Part 3: From Mechanistic Affiliation to Origin Inference, in: *Modern Magnetic Resonance*, edited by Webb, G. A., pp. 1669–1680, Springer Netherlands, doi:10.1007/1-4020-3910-7_187, 2006a.
- Martin, M., Zhang, B., and Martin, G. J.: SNIF-NMR—Part 2: Isotope Ratios as Tracers of Chemical and Biochemical Mechanistic Pathways, in: *Modern Magnetic Resonance*, edited by Webb, G. A., pp. 1659–1667, Springer Netherlands, doi:10.1007/1-4020-3910-7_186, 2006b.
- Shilling, J. E., Chen, Q., King, S. M., Rosenørn, T., Kroll, J. H., Worsnop, D. R., McKinney, K. A., and Martin, S. T.: Particle mass yield in secondary organic aerosol formed by the dark ozonolysis of alpha-pinene, *Atmos. Chem. Phys.*, 8, 2073–2088, doi:10.5194/acp-8-2073-2008, www.atmos-chem-phys.net/8/2073/2008/, 2008.

- Silvestre, V., Mboula, V. M., Jouitteau, C., Akoka, S., Robins, R. J., and Remaud, G. S.: Isotopic ^{13}C NMR spectrometry to assess counterfeiting of active pharmaceutical ingredients: Site-specific ^{13}C content of aspirin and paracetamol, *J. Pharmaceut. Biomed.*, 50, 336–341, doi:10.1016/j.jpba.2009.04.030, <http://www.sciencedirect.com/science/article/pii/S0731708509002738>, 2009.
- Tani, A., Hayward, S., and Hewitt, C.: Measurement of monoterpenes and related compounds by proton transfer reaction-mass spectrometry (PTR-MS), *Int. J. Mass Spectrom.*, 223–224, 561–578, doi:10.1016/S1387-3806(02)00880-1, <http://www.sciencedirect.com/science/article/pii/S1387380602008801>, 2003.
- Tenailleau, E. and Akoka, S.: Adiabatic ^1H decoupling scheme for very accurate intensity measurements in ^{13}C NMR, *J. Magn. Reson.*, 185, 50–58, doi:10.1016/j.jmr.2006.11.007, <http://linkinghub.elsevier.com/retrieve/pii/S1090780706003818>, 2007.
- VanReken, T. M., Ng, N. L., Flagan, R. C., and Seinfeld, J. H.: Cloud condensation nucleus activation properties of biogenic secondary organic aerosol, *J. Geophys. Res.*, 110, D07206, doi:10.1029/2004JD005465, <http://www.agu.org/pubs/crossref/2005/2004JD005465.shtml>, 2005.
- Zelenyuk, A., Yang, J., Song, C., Zaveri, R. A., and Imre, D.: A New Real-Time Method for Determining Particles' Sphericity and Density: Application to Secondary Organic Aerosol Formed by Ozonolysis of alpha-Pinene, *Environ. Sci. Technol.*, 42, 8033–8038, doi:10.1021/es8013562, <http://pubs.acs.org/doi/pdf/10.1021/es8013562>, 2008.